Communications on Applied Nonlinear Analysis
ISSN: 1074-133X
Vol 32 No. 9s (2025)

Enhanced Accuracy in Cellular Automata-Markov Chain Model for Land Classification Analysis and Prediction

Susanta Kundu[1], Ashima Rani [2], Vinod Kumar [3]

1 Department of Computer Science, Faculty of Engineering and Technology, SGT University, Gurgaon, India 122005
susanta_feat@sgtuniversity.org
2 Department of Computer Science, Faculty of Engineering and Technology, SGT University, Gurgaon, India 122005
ashima_feat@sgtuniversity.org
3 Retired Professor, Department of Computer Science, Faculty of Engineering and Technology, SGT University
gvkssun@gmail.com

Article History:

Received: 12-11-2024

Revised: 22-12-2024

Accepted: 18-01-2025

Abstract:
Technology can leverage green solutions with Land Classification (LC) analysis and prediction to promote sustainable land management, paving its way to eco-centric development by analyzing hyper-spectral satellite images for land classification using machine learning (ML) techniques and predicting future trends with improved accuracy. LC-ML synergy aligns with green technology to monitor deforestation, habitat destruction, and climate change. Improved accurate land classification and prediction assist in sustainable land resource management and optimization. It supplements data-driven insights into urban planning and eco-friendly infrastructure development by identifying areas for reforestation relating to carbon sequestration and renewable energy integration. Sustainable management of agricultural land, forests, urban areas, and water bodies can prevent resource depletion from controlling environmental degradation. Accurate land cover predictions over 30 years can help policymakers avoid resource depletion and promote sustainability. This study analyzed historical data for LC classification and then used the Cellular Automata Markov Chain (CA-MC) model to predict future trends. Model reliability is assessed by metrics such as the Kappa and overall accuracy. With an overall model accuracy of 81.33%, these refinements contribute to policymakers' decision-making to plan sustainable land use, allocate resources, and balance environmental conservation with economic development. The model supports stakeholders in identifying LC patterns, particularly in urban expansion and deforestation, to promote equitable and sustainable growth.

Keywords: Green Technology, State Transition Matrix, Kappa, Sustainability

1 Introduction

Green technology incorporates eco-friendly solutions like renewable energy, carbon sequestration, and sustainable infrastructure that can rely on Land Classification (LC) data accuracy. LC supports green technology by identifying suitable areas for solar farms and regions for reforestation to boost carbon sequestration. Improved accuracy helps urban planners design green spaces to reduce the urban heat island effect and enhance biodiversity. LC accuracy land use changes aid long-term planning, balancing economic growth, social equity, and environmental conservation. Predicting changes over the next 30 years provides crucial insights for greener planning based on informed decisions. The projected model, which clustered land into agriculture, forest, urban, and water, forms an impactful classification [1]. Historical land data for thirty years is trained to estimate future changes and promote community engagement as an alternative conservation strategy [2]. The CA-MC model predicts LC changes stochastically, where the current *state(t)* depends on *state(t-1)*. A State Transition Matrix (STM), a derivative of the confusion matrix, forecasts changes based on available data [3]. The STM elements represent the pixel probability of continuing the same state or change [4]. The model accuracy influences the effectiveness of policy development to balance economic growth and resource conservation.

The literature survey reviewed LC models whose accuracy depends on data, configurations, and STM matrix element values. The review finds a gap in realistic interpretations of non-diagonal elements of STM, as most studies focused only on the diagonal elements (treating TRUE) to assess the accuracy. This study improves the CA-Markov model by redefining certain non-diagonal elements of the STM as valid land transitions, such as forest-to-urban or forest-to-agriculture. Transitions like land-to-urban or land-to-water are included to enhance accuracy. These improvements support green technology by helping policymakers plan for renewable energy, carbon sequestration, and sustainable urban spaces. By refining land transition predictions, the study promotes eco-conscious decision-making and more precise land use planning.

2 Objectives

The study explores the spatial-temporal land changes categorized into (1) land, (2) urban, (3) forest, and (4) water bodies. These four categories capture the essential components of the Earth’s surface that directly influence ecological balance and serve as sustainability indicators. They represent key components of the Earth’s surface that impact ecological balance and act as sustainability indicators [5]. Land includes open spaces, agricultural fields, and crops, essential for monitoring soil health and supporting sustainable farming practices with green technologies. Forests serve as biodiversity hubs and carbon sinks, helping track deforestation, reforestation, and carbon storage to support carbon-neutral goals. Urban areas reflect population and infrastructure growth, highlighting energy and resource demands that are addressable with renewable and energy-efficient technologies. Water bodies—such as lakes, rivers, and wetlands—are vital for freshwater supply, flood control, and ecosystem health, with green technologies aiding in water conservation and management. It emphasizes predictive modelling and accuracy improvements to help policymakers curb urban sprawl, adopt eco-friendly solutions, and protect forests and farmland for a sustainable future.

3 Methods

The clusters created by the unsupervised classification k-means, for k=30, were reclassified into (1) Agriculture (AGR), (2) Forest (FOR), (3) Urban (URB), and (4) Water (WAT) bodies. AGR includes crops, sowing, and empty diverse land. FOR broadly covers natural forests, cultivated plantations, managed horticulture areas, etc. These are approximately higher than 5m, with a canopy of 10% reaching these dimensions [6]. URB is built-up areas including residential, industrial, and factory sheds, roads, etc. WAT includes rivers, lakes, canals, and natural or artificial reservoirs. These four categories influence ecological balance and serve as sustainability indicators. Their changes in 1994 and 2024 are the basis of training the model. LC changes projected for 2054 using this model offer future insights into urbanization, water body patterns, and changes in land and forest.

LC Prediction

Leveraging historical data and probabilistic rules, the prediction model captures LC transformations outlined by the CA-MC model. The equation defining the Cellular Automata (CA) model used in this study is

$$C(t,t+1) = R(C(t),n), \text{ where:}$$

C = state; n = classification count; t, and (t + 1) are successive moments; R = state change rule [6].

The MC model estimates LC changes driven by conditional probability,

$$C(t + 1) = P_{ij} * C(t) \text{ where:}$$

C(t), and C(t + 1) are independent consecutive states, P_{ij} = STM calculated by,

$$P_{ij} = \begin{bmatrix} P_{11} & \cdots & P_{1n} \\ \vdots & \vdots & \vdots \\ P_{n1} & \cdots & P_{nn} \end{bmatrix}, where \sum_{j=i}^{n} \left(P_{ij}\right) = 1 \text{ ; i and j are LU types.}$$

The transition matrix P_{ij} value (either 0 or 1) indicates the state change probabilities [7]. The transition of a cell state examines the spatial relationships with adjoining cells to update its state [8]. In this framework, neighbourhood pixels are external factors that influence the state transitions of a pixel [9]. It generates a simulated change map 2054, using the 1994-2024 changes as a reference[10].

Accuracy Assessment

The overall accuracy is the ratio between observed and chance classifications. K, the Kappa Coefficient quantifies the accuracy of classifications by comparing observed variables with predicted classifications. It is represented by,

$$K = [P(a) – P(e)] / [1 – P(e)], \text{ where}$$

P(a) = chance of correctly observed classification, and P(e) = chance of predicting the classified pixel [11].

Data Collection

Gurgaon district in Haryana - India, was selected for this study due to its rapid transformation from an agricultural region to an urbanized hub. Figure 1 highlights the area of interest (inset) in India. It represents broader global trends in urban expansion, particularly in the developing regions where economic growth and population pressures drive significant land-use changes. For example, Kenya in Nairobi experienced rapid urban spread driven by population growth and economic opportunities [12]. Similarly, the Pearl River Delta is a globally recognized example of urban-industrial transformation [13]. In Sao Paulo, urban growth extended into peripheral areas, creating challenges in infrastructure, housing, and green space preservation [14]. This study uses Landsat satellite images for land classification to predict changes after thirty years. A search on EarthExplorer by USGS [15] identified Landsat images based on (1) acquisition dates (between March to May of 1994 and 2024), (2) Gurgaon district contour as the study area, and (3) less than 5% cloud cover. The satellite scenes have 30-meter spatial resolutions, each covering 900m x 900m land surface with WRS path and row information.

Various band combinations are used in the study for false-coloured images to display different land cover types required in data validation.

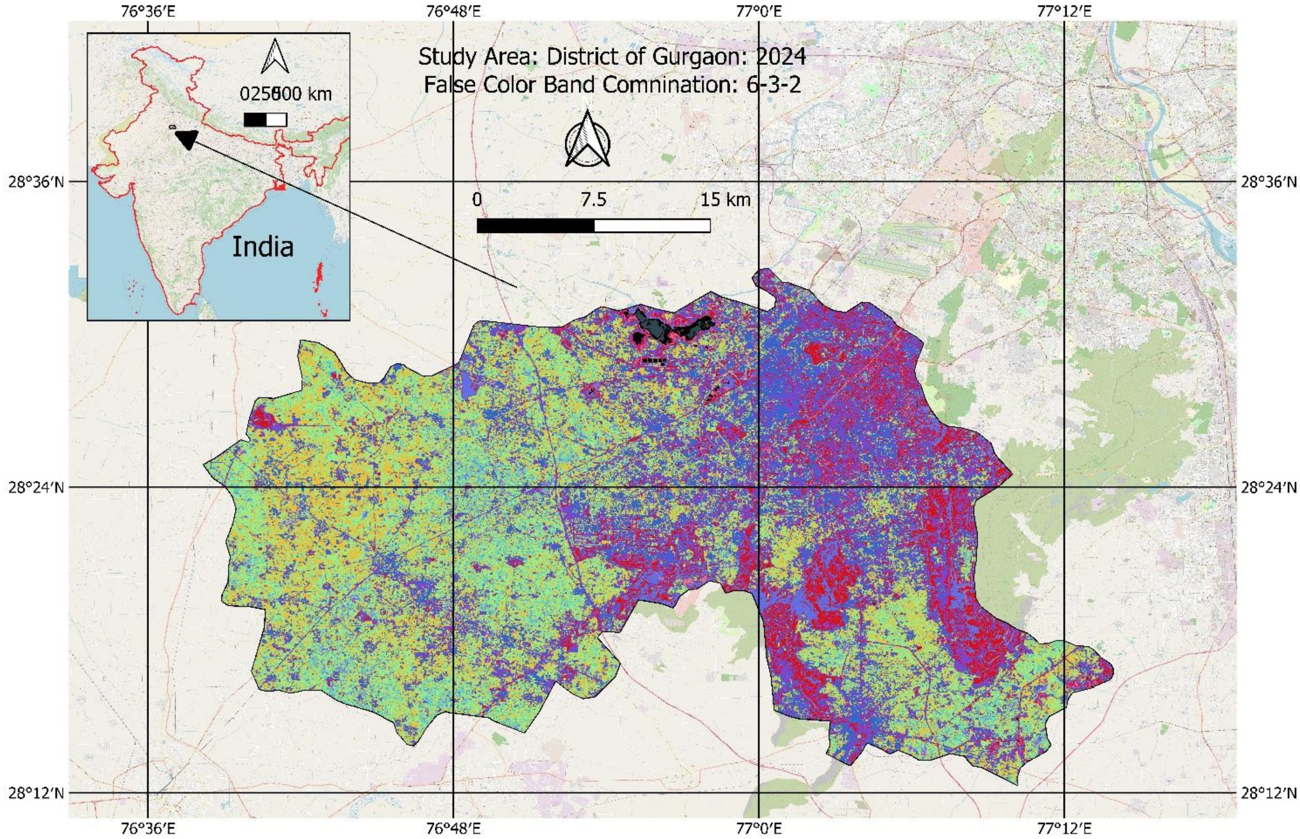

Figure 1. Study Area – Location Map

The resulting images with path/row information in Table 1 have minimal time gaps between acquisitions. Geometric corrections applied by USGS using the Dark Object Subtraction (DOS) procedure [16] were available with data.

Table 1. Landsat Scenes Used for LC Classification

#	Landsat Scene Identifier	Acquired	Path	Row	CC*
1	LC81460412024097LGN00	2024-04-07	146	41	0.3
2	LC81470402024104LGN00	2024-04-14	147	40	0.5
3	LT05_L1TP_146040_19940507_20200814_02_T1	1994-05-07	146	40	0
4	LT05_L1TP_17040_19940512_20200814_02_T1	1994-05-12	147	40	0

* Cloud Coverage

The relevant two satellite scene pairs (1, 2, and 3, 4) from Table 1 were mosaicked for the study area and then cropped according to a contour to create the region of interest.

4 Results

The findings highlight the predicted LC changes from 2024 to 2054, presented through maps and statistical summaries. K-means unsupervised ML model was applied with k = 30 to produce 30 clusters. They were subjected to a supervised ML model to reclassify into Land, Forest, Urban, and Water [17]. The accuracy assessment uses OA, UA, PA, and the kappa coefficient. The model generated the LC Classification maps of the study area (district Gurgaon) in Figure 2 and Figure 3 for 1994 and 2024, respectively.

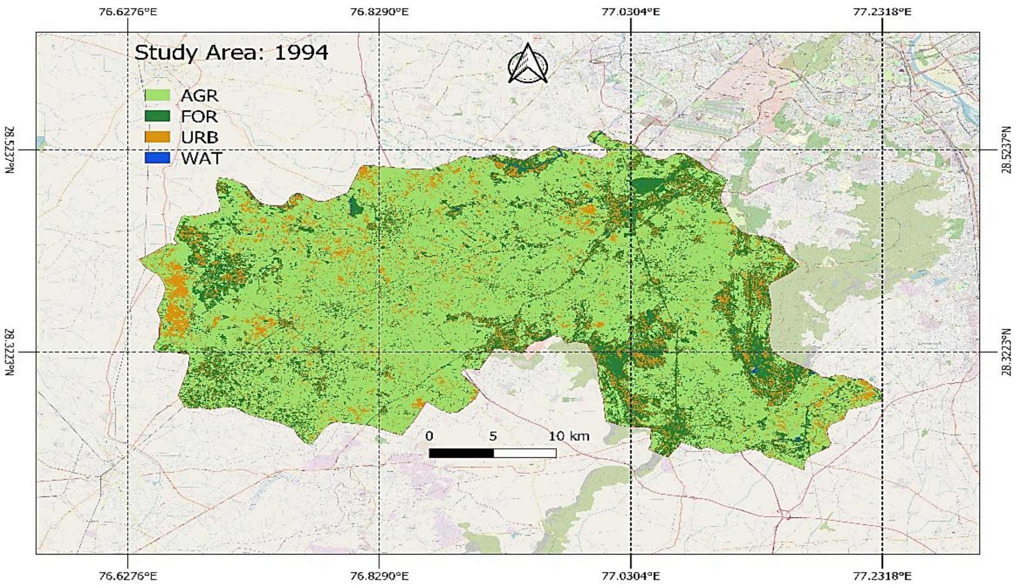

Figure 2: Land Classification Map: 1994 (k=4)

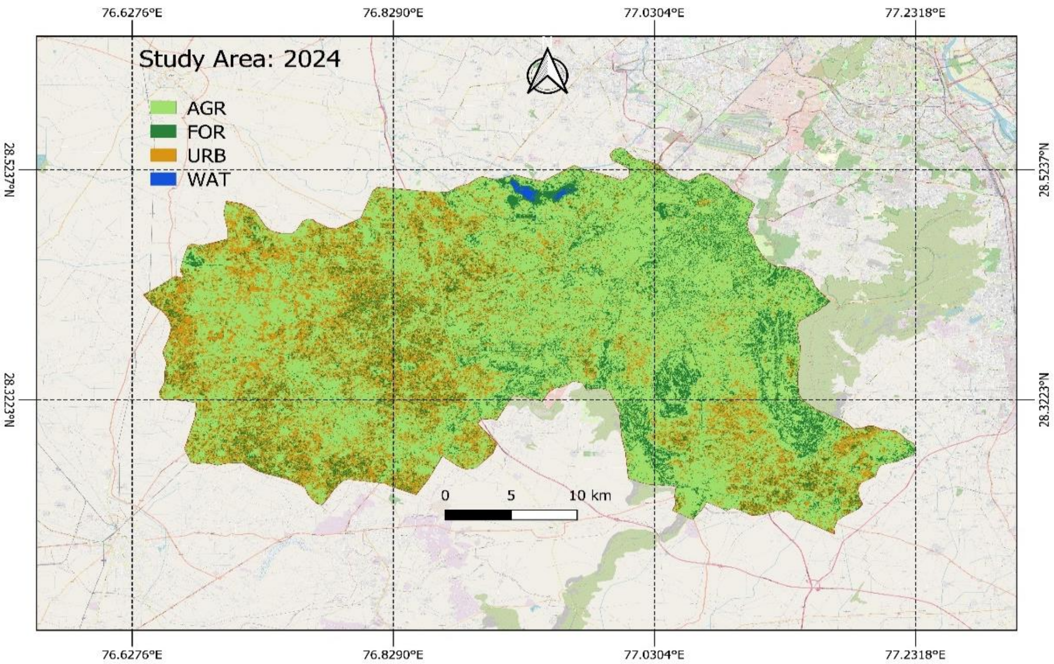

Figure 3: Land Classification Map: 2024 (k=4)

Class statistics

Class statistics is the quantitative measure of each classification [18] to understand the dynamics of LC, making them relevant for sustainable development and resource management. [19]. The selection of four land classifications can be coarse for applications with finer resolution or granularity. However, they adequately provide consistency in long-term trends and policy-framing goals, supporting informed decisions for sustainable land management and planning. The detailed class statistics of the study areas are in Table 2 for changes in 1994 and 2024. Land (LAN) decreased from 67.84% in 1994 to 62.22% in 2024, a decline of –5.62%. Forest (FOR) declined from 19.57% in 1994 to 16.27% in 2024, indicating a decrease of 3.3%. Urban areas had an 8.89% rise, growing from 12.46% in 1994 to 21.35% in 2024. Population growth and economic development drove the increase in urban areas. Water Bodies showed a marginal increase, rising from 0.13% in 1994 to 0.16% in 2024. The change may be due to the improved water management practices.

Table 2. Land Usage per cent distributions in 1994 and 2024

Temporal State	Year	LAN (%)	FOR (%)	URB (%)	WAT (%)	Total (%)
Initial (I)	1994	67.84	19.57	12.46	0.13	100
Final (F)	2024	62.22	16.27	21.35	0.16	100
Δ % (F – I)		-5.62	-3.3	8.89	0.03	

Figure 4 is the change map from 1994 to 2024, which indicates the thirty-year land transformation. The change of information is used to model the simulated map in 2054.

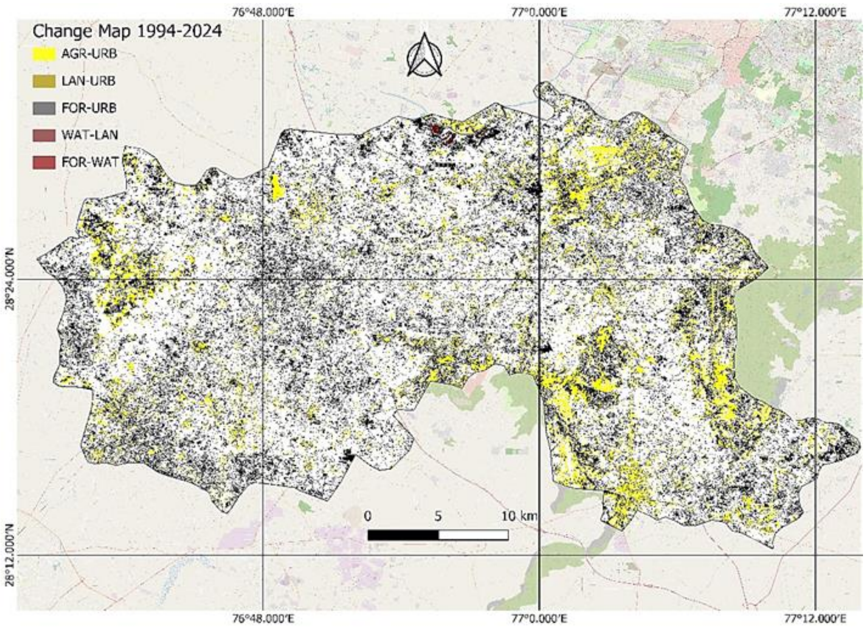

Figure 4: Land Classification Change Map from 1994 to 2024

State Transition Matrix (STM)

The STM has transition elements outlining the likelihood of one class transitioning to another between successive time intervals. Table 3 is the STM of the study area maps for 1994 and 2024, used to predict the LC map for 2054. Overall Accuracy (OA) is calculated by summing the diagonal elements.

The study, as its novelty, treated specific state transitions in non-diagonal elements as valid transitions. Transitions from FOR to LAN or FOR to URB are valid examples of deforestation to improve the model's accuracy.

Table 3. STM (1994-2024) for Predicting Land Use Changes by 2054

Final 2024	Initial 1994 (→)				
(↓)	AGR (%)	FOR (%)	URB (%)	WAT (%)	Total (%)
AGR	41.42	13.51	7.29	0.07	62.22
FOR	9.45	4.10	2.68	0.04	16.27
URB	16.98	1.87	2.44	0.005	21.35
WAT	0.03	0.06	0.07	0.0001	0.16
Total	67.84	19.57	12.46	0.13	100
UA [%]	66.51	25.17	11.45	0.48	
PA [%]	61.02	20.96	19.54	0.65	
OA [%]	81.33				
Kappa	0.64				

Validation

The study selected random points to represent LC classes, validated them with Google Maps, and verified them against published data, as shown in Table 4, including government reports from 2000 and 2008. Although this approach has limitations, it provides a practical alternative when field-based data validation is unavailable.

Table 4. LC Classification distribution (%)

Year	Source	AGR (%)	FOR (%)	URB (%)	WAT (%)	Total (%)
1994	Landsat	67.84	19.57	12.46	0.13	100
2000	* Gov. Report	69.79	18.81	10.92	0.58	100
2008	* Gov. Report	65.57	19.18	15.07	0.16	100
2024	Landsat	62.22	16.27	21.35	0.16	100

* Department of Town and Country Planning, Haryana. ([20])

Accuracy Assessment

Accuracy Assessment ensures models reflect near real-world conditions. It minimizes decision errors to reduce economic and environmental risks. A reliable classification model can be applied to other regions with minimal reconfiguration, ensuring transferability. This study predicts the LC classification map 2054 using the ANN-MLP algorithm [21], with parametric values in Table 5. The MOLUSE plug-in of QGIS derived trained data in 1994 and 2024 to simulate trends in 2054, which is essential for understanding and predicting land cover changes.

Table 5. Model Configuration Parameters Used in ANN – MLP

Parameter	Value
Neighborhood (pixel)	1
Learning Rate	0.1
Maximum Iterations	1000
Hidden Layers	10
Momentum	0.05
Number of simulation iterations	5

The configuration parameters are effective in learning, model convergence, and prediction. Neighborhood (pixel) = 1 processes the spectral characteristics of individual pixels. Learning Rate = 0.1 avoids overshooting the optimal solution with stable weight updates during backpropagation. Maximum Iterations = 1000 ensures sufficient time for the model to learn the input data patterns and avoid premature termination. Hidden Layers = 10 captures the nonlinear relationships between spectral signatures of land cover classes for extracting higher-order features. Momentum = 0.5 smoothens the optimization process, ensuring stability during weight updates without overriding the effect of the learning rate.

The spatial accuracy assessment used random sampling across all LC classifications to ensure balanced representation. The matrices like Kappa (0.993) assessed spatial misclassifications and validated between predicted and reference classifications. The minimum validation error (0.00007) indicates that the model generalizes well to unseen data. Table 6 shows transitions between 2024 and 2054 (simulated).

Table 6. Transition Matrix Comparing 2024 with 2054 (Simulated)

	Initial 2024 (→)				
Final 2054 (↓)	AGR (%)	FOR (%)	URB (%)	WAT (%)	Total (%)
AGR	62.25	0.03	0.0075	0.0021	62.29
FOR	0.01	14.53	0.03	0.0024	14.59
URB	0.007	1.71	21.24	0.0182	22.98
WAT	0.0019	0.001	0.0006	0.13	0.14
Total	62.22	16.27	21.35	0.16	100
UA [%]	99.95	99.77	99.96	98.29	
PA [%]	99.97	89.53	99.96	99.97	
OA	98.25% (Correctly Classified Pixel / Total Pixels)				
Kappa	0.96 (Probability of chance agreement)				

It captures changes predicted after 30 years, acknowledging a finer spatial or temporal detail might be required for localized studies and applications [22]. The vast area covered has limitations of ground truth data and the availability of open-source high-resolution satellite images to substantiate model training. Figure 5 is the LC map of the study area 2054 (simulated). It can provide input to balance the need to preserve natural resources for sustainability [23]. The reduction in water bodies is minor. The changes in the LC patterns might bring economic benefits but pose infrastructure challenges [24].

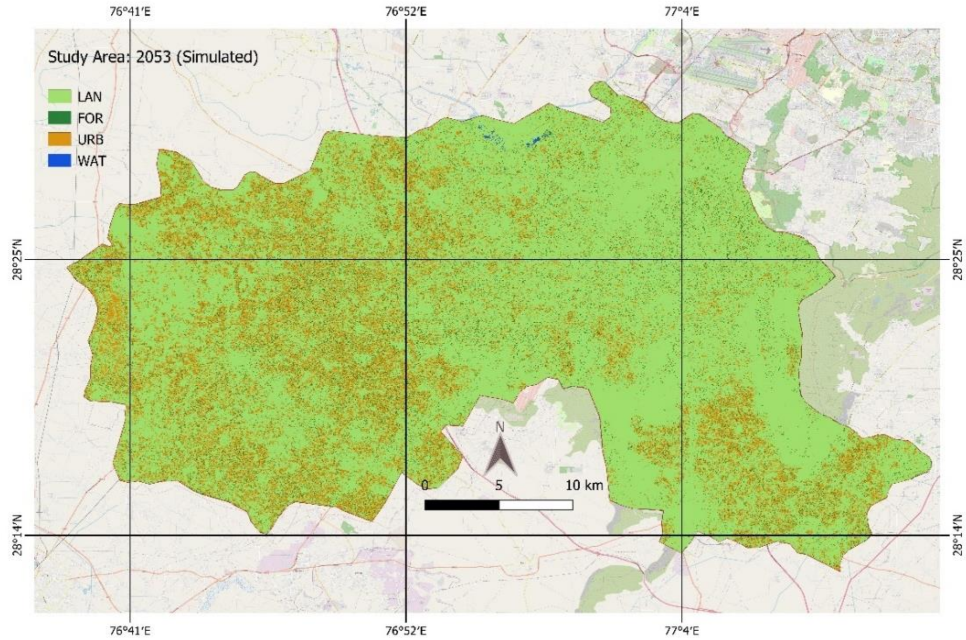

Figure 5. LC Classification of Predicted Map (2054)

Accuracy assessment has a few challenges. Similar spectral signatures of LC types may cause misclassification, as pixels may contain multiple types, reducing precision [25]. Imbalanced LC classes affect the model accuracy. Imbalanced LC classes occur when some land cover types have more samples, leading to biased models [26]. Temporal variability due to seasonal changes can alter land cover appearance, leading to misclassification. The referenced data errors in ground truth data can lead to incorrect accuracy assessments. Integrated techniques in ML, feature reduction methods, and high-quality reference data can improve classification precision, leading to more reliable land management decisions.

5 Discussion

The findings reveal key trends in land cover changes and their impact on sustainability. Comparing results with existing data helps assess model accuracy in integrating green technology to improve prediction capabilities in land management. Such limitations can refine future research and policy decisions as potential improvements.

Scalability

Scaling LC models from the study area to broader regions or national and global levels involves several challenges. It has technical limitations, data availability, resource constraints, and alignment with policy frameworks. ML and simulation models become computationally expensive when applied to larger datasets with finer resolution and an extensive area. Such regions may have inconsistent historical and limited ground-truth data and need to explore alternative or crowd-sourced data.

With increased data volume, ML processing becomes complex and ineffective. Algorithms like CNN and RF require significant computing power to process high-resolution images for training and analysis. [27]. Managing large datasets will also require high-capacity advanced storage solutions and distributed file systems, adding operational complexity [28]. Parallel computing frameworks [27] can ease scalability challenges. Table 7 summarizes key scalability challenges and related impacts.

Table 7: Scalability Challenges

Challenges	Example	Constraint
High-resolution images need higher memory and processing power.	~100,000 km² data in Deep Learning needs 5–10 times more memory [29].	Computational Constraint
DL models require extensive training in high-dimensional data.	Ten times image resolution can increase training time by 8-12 times [30].	Algorithmic Complexity

Scalability in cloud-based computing enables efficient processing of large LC datasets. Parallel deep learning speeds up training, reducing computation time by 50-80% for global-scale LC classification. Scalability also increases prediction uncertainties due to sensor noise, missing data spectral variability, and mixing overlapping spectral signatures, which all add classification errors in heterogeneous landscapes [31]. Moreover, a model trained in one region may not perform well in another due to differences in climate, vegetation, and land-use patterns. Future predictions may not account for unforeseen climate events, land-use policies, or socio-economic changes affecting land cover. Scalability challenges and prediction errors can lead to misclassified land types, causing outdated information and unreliable zoning or conservation decisions by policymakers.

Error Margin

Error margins in LC classification accuracy vary based on data resolution, classification methods, and other complexities. Understanding these margins helps to improve model accuracy by selecting classification techniques, training data, and integrating high-resolution images. Table 8 has an error margin in critical areas of LC accuracy assessment.

Table 8: Error Margin of influencing factors in LC classification

Influencing Factors	Impact on	EM
1. Image resolution (higher resolution reduces error) 2. LC classes (more classes increase complexity) 3. Training data quality [32]	OA	±2% to ±10%
1. Dataset size (larger training sets reduce error) 2. Class proportion (balanced data improve stability) [25]	Kappa	±0.05 to ±0.15
1. Similar LC reflectance (example: bare soil vs. urban) 2. Sensor resolution (reduces spectral overlap) [33]	Spectral Mixing	±5% to ±15%
1. Lower resolution increases uncertainty 2. LC heterogeneity (fragmented landscape errors) [34]	Pixel Resolution	±5% to ±10%

* EM (Error Margin)

The simulated 2054 forecast has uncertainties with an error margin that accounts for influencing it. The expected overall error margin can range between 5-15%, depending on the accuracy of input data and assumptions.

Socio Economy

Lesser image resolution helps to identify smaller-scale urbanization and forest areas. Errors in the preprocessing phase and misclassification due to spectral mixing propagate into the model prediction error. Reliability and accuracy thus depend on the data quality used to derive the STM, but its transition probabilities might not account for socio economic or environmental changes. It also ignores policy interventions or technological advancement. The prediction accuracy declines with increased prediction interval [35]. The validation process uses historical government reports, observed data, and satellite images. Errors or inaccuracies in these sources can impact model predictions [36]. Addressing predicted losses of forests and water bodies is essential for ecological balance and long-term sustainability. Green technology can improve prediction accuracy and support sustainable urban planning through remote sensing and AI monitoring. Urban development should focus on green technology-driven cities for reduced environmental impacts to promote eco-friendly infrastructure.

Potential Improvement

The study observed LC land changes degrade ecosystems and biodiversity. Integrating green technology for renewable energy, water conservation systems, and pollution control technologies can help mitigate these impacts. Development processes can also address socio-economic disparities and promote inclusive growth by adopting equitable, eco-friendly land use practices in the district, ensuring a balance between development and environmental sustainability. Policymakers must overcome scalability challenges, especially by working with government agencies to access administrative datasets, socio-economic statistics, and ground-truthing information. Leveraging green technology in AI-driven environmental monitoring, renewable energy-powered data centres, and remote sensing innovations, enhanced data accuracy will promote sustainable practices.

Global organizations like NASA, ESA, USGS, and ISRO can provide high-quality satellite imagery to support detailed environmental analysis. Private-sector technology firms can offer advanced computing infrastructure and green technology solutions to drive efficient, eco-friendly land use and sustainable urban planning.

The study integrated complex data to predict changes using green technology, like AI-driven monitoring and remote sensing images, to improve prediction accuracy. The enhanced LC model helps to translate research into actionable insights for sustainable land-use planning and policymaking. Continued study with green technology is essential to improve model accuracy for enhanced reliability of a scalable complex system.

References

[1] S. Singh and R. Biswas, “Analysis of Land Use Change Effects/Impacts on Surface Water Resources in Delhi,” *Urban Science*, vol. 6, no. 4, p. 92, Dec. 2022, doi: 10.3390/urbansci6040092.

[2] P. Subedi, K. Subedi, and B. Thapa, "Application of a Hybrid Cellular Automaton – Markov (CA-Markov) Model in Land-Use Change Prediction: A Case Study of Saddle Creek Drainage Basin, Florida," *AEES*, vol. 1, no. 6, pp. 126–132, Nov. 2013, doi: 10.12691/aees-1-6-5.

[3] Md. S. Mondal, N. Sharma, P. K. Garg, and M. Kappas, "Monitoring and Spatially Explicit Simulation of Land Use Dynamics: From Cellular Automata to Geosimulation - A Case Study of Tehran, Iran," *The Egyptian Journal of Remote Sensing and Space Science*, vol. 19, no. 2, pp. 259–272, Dec. 2016, doi: 10.1016/j.ejrs.2016.08.001.

[4] J. J. Arsanjani, W. Kainz, and M. Azadbakht, "Monitoring and Spatially Explicit Simulation of Land Use Dynamics: From Cellular Automata to Geosimulation - A Case Study of Tehran, Iran," in *2011 International Symposium on Image and Data Fusion*, Tengchong, Yunnan, China: IEEE, Aug. 2011, pp. 1–4. doi: 10.1109/ISIDF.2011.6024203.

[5] H. Qiu, J. Zhang, H. Han, X. Cheng, and F. Kang, "Study on the impact of vegetation change on ecosystem services in the Loess Plateau, China," *Ecological Indicators*, vol. 154, p. 110812, Oct. 2023, doi: 10.1016/j.ecolind.2023.110812.

[6] T. Tokihiro, D. Takahashi, J. Matsukidaira, and J. Satsuma, "From Soliton Equations to Integrable Cellular Automata through a Limiting Procedure," *Phys. Rev. Lett.*, vol. 76, no. 18, pp. 3247–3250, Apr. 1996, doi: 10.1103/PhysRevLett.76.3247.

[7] R. G. Pontius and L. C. Schneider, "Land-cover change model validation by an ROC method for the Ipswich watershed, Massachusetts, USA," *Agriculture, Ecosystems & Environment*, vol. 85, no. 1–3, pp. 239–248, Jun. 2001, doi: 10.1016/S0167-8809(01)00187-6.

[8] E. Koomen and J. A. M. Borsboom van Beurden, Eds., *Land-use modelling in planning practice*. in The GeoJournal library, no. v. 101. New York: Springer, 2011.

[9] R. Hamad, H. Balzter, and K. Kolo, "Predicting Land Use/Land Cover Changes Using a CA-Markov Model under Two Different Scenarios," *Sustainability*, vol. 10, no. 10, p. 3421, Sep. 2018, doi: 10.3390/su10103421.

[10] B. Markham *et al.*, "Landsat-8 Operational Land Imager Radiometric Calibration and Stability," *Remote Sensing*, vol. 6, no. 12, pp. 12275–12308, Dec. 2014, doi: 10.3390/rs61212275.

[11] Mary L. McHugh, "Interrater reliability: the kappa statistic," *Biochemia Medica*, pp. 276–282, Oct. 2012.

[12] C. N. Mundia and M. Aniya, "Analysis of land use/cover changes and urban expansion of Nairobi city using remote sensing and GIS," *International Journal of Remote Sensing*, vol. 26, no. 13, pp. 2831–2849, Jul. 2005, doi: 10.1080/01431160500117865.

[13] K. C. Seto, R. K. Kaufmann, and C. E. Woodcock, "Monitoring Land Use Change in the Pearl River Delta, China," in *Linking People, Place, and Policy*, S. J. Walsh and K. A. Crews-Meyer, Eds., Boston, MA: Springer US, 2002, pp. 69–90. doi: 10.1007/978-1-4615-0985-1_4.

[14] G. N. D. Lima and V. O. Magaña Rueda, "The urban growth of the metropolitan area of Sao Paulo and its impact on the climate," *Weather and Climate Extremes*, vol. 21, pp. 17–26, Sep. 2018, doi: 10.1016/j.wace.2018.05.002.

[15] USGS, "EarthExplorer - USGS." [Online]. Available: https://earthexplorer.usgs.gov/

[16] Z. Zhang, G. He, and X. Wang, "A practical DOS model-based atmospheric correction algorithm," *International Journal of Remote Sensing*, vol. 31, no. 11, pp. 2837–2852, Jun. 2010, doi: 10.1080/01431160903124682.

[17] M. Wang, L. Cai, H. Xu, and S. Zhao, "Predicting land use changes in northern China using logistic regression, cellular automata, and a Markov model," *Arab J Geosci*, vol. 12, no. 24, p. 790, Dec. 2019, doi: 10.1007/s12517-019-4985-9.

[18] J. F. Gondwe, S. Lin, and R. M. Munthali, "Analysis of Land Use and Land Cover Changes in Urban Areas Using Remote Sensing: Case of Blantyre City," *Discrete Dynamics in Nature and Society*, vol. 2021, pp. 1–17, Dec. 2021, doi: 10.1155/2021/8011565.

[19] S. Madusanka, C. Abenayake, A. Jayasinghe, and C. Perera, “A Decision-Making Tool for Urban Planners: A Framework to Model the Interdependency among Land Use, Accessibility, Density, and Surface Runoff in Urban Areas,” *Sustainability*, vol. 14, no. 1, p. 522, Jan. 2022, doi: 10.3390/su14010522.

[20] Scott Wilson India Private Limited, “Preparation of Sub Regional Plan for Haryana Sub-Region of NCR-2021.” Department of Town and Country Planning, Haryana, Sep. 2010. [Online]. Available: https://www.smsfoundation.org/wp-content/themes/sehgal/pdf/Draft%20Final%20Report-Haryana%20Sub-Regional%20Plan%202021.pdf

[21] B. Sajan, V. N. Mishra, S. Kanga, G. Meraj, S. K. Singh, and P. Kumar, “Cellular Automata-Based Artificial Neural Network Model for Assessing Past, Present, and Future Land Use/Land Cover Dynamics,” *Agronomy*, vol. 12, no. 11, p. 2772, Nov. 2022, doi: 10.3390/agronomy12112772.

[22] D. Tilahun, K. Gashu, and G. T. Shiferaw, “Effects of Agricultural Land and Urban Expansion on Peri-Urban Forest Degradation and Implications on Sustainable Environmental Management in Southern Ethiopia,” *Sustainability*, vol. 14, no. 24, p. 16527, Dec. 2022, doi: 10.3390/su142416527.

[23] N. Cuong Huu, Cuong Van, and Tien My Ngoc, “Monitoring and Modeling of Spatio-Temporal Urban Expansion and Land Use/Land-Cover Change in Mountain Landscape: A Case Study of Dalat City, Vietnam,” *Environ. Nat. Resour. J.*, vol. 21, no. 5, pp. 1–15, Sep. 2023, doi: 10.32526/ennrj/21/20230086.

[24] A. Razali, S. N. Syed Ismail, S. Awang, S. M. Praveena, and E. Zainal Abidin, “Land use change in highland area and its impact on river water quality: a review of case studies in Malaysia,” *Ecol Process*, vol. 7, no. 1, p. 19, Dec. 2018, doi: 10.1186/s13717-018-0126-8.

[25] A. Adhikari, H. B. Menon, and A. Lotliker, “Coupling of hydrography and bio-optical constituents in a shallow optically complex region using ten years of in-situ data,” *ISPRS Journal of Photogrammetry and Remote Sensing*, vol. 202, pp. 499–511, Aug. 2023, doi: 10.1016/j.isprsjprs.2023.07.014.

[26] S. Kumar, Shwetank, and K. Jain, “A Multi-Temporal Landsat Data Analysis for Land-use/Land-cover Change in Haridwar Region using Remote Sensing Techniques,” *Procedia Computer Science*, vol. 171, pp. 1184–1193, 2020, doi: 10.1016/j.procs.2020.04.127.

[27] G. Cavallaro *et al.*, “Scalable developments for big data analytics in remote sensing,” in *2015 IEEE International Geoscience and Remote Sensing Symposium (IGARSS)*, Milan, Italy: IEEE, Jul. 2015, pp. 1366–1369. doi: 10.1109/IGARSS.2015.7326030.

[28] A. M. Burgueño *et al.*, “Scalable approach for high-resolution land cover: a case study in the Mediterranean Basin,” *J Big Data*, vol. 10, no. 1, p. 91, Jun. 2023, doi: 10.1186/s40537-023-00770-z.

[29] I. A. T. Hashem, I. Yaqoob, N. B. Anuar, S. Mokhtar, A. Gani, and S. Ullah Khan, “The rise of ‘big data’ on cloud computing: Review and open research issues,” *Information Systems*, vol. 47, pp. 98–115, Jan. 2015, doi: 10.1016/j.is.2014.07.006.

[30] N. Summers, G. Johnsen, A. Mogstad, H. Løvås, G. Fragoso, and J. Berge, “Underwater Hyperspectral Imaging of Arctic Macroalgal Habitats during the Polar Night Using a Novel Mini-ROV-UHI Portable System,” *Remote Sensing*, vol. 14, no. 6, p. 1325, Mar. 2022, doi: 10.3390/rs14061325.

[31] Z. Li, B. Chen, S. Wu, M. Su, J. M. Chen, and B. Xu, “Deep learning for urban land use category classification: A review and experimental assessment,” *Remote Sensing of Environment*, vol. 311, p. 114290, Sep. 2024, doi: 10.1016/j.rse.2024.114290.

[32] M. Chen *et al.*, “A Motion Compensation Method for Shipborne HFSWR by Using Dual Reference RF Signals Generated Onshore,” *Remote Sensing*, vol. 14, no. 5, p. 1055, Feb. 2022, doi: 10.3390/rs14051055.
[33] H. Li, S. Jia, and Z. Le, “Prediction of Soil Organic Carbon in a New Target Area by Near-Infrared Spectroscopy: Comparison of the Effects of Spiking in Different Scale Soil Spectral Libraries,” *Sensors*, vol. 20, no. 16, p. 4357, Aug. 2020, doi: 10.3390/s20164357.
[34] S. V. Stehman, “Estimating area from an accuracy assessment error matrix,” *Remote Sensing of Environment*, vol. 132, pp. 202–211, May 2013, doi: 10.1016/j.rse.2013.01.016.
[35] M. M. Aburas, Y. M. Ho, M. F. Ramli, and Z. H. Ash’aari, “Improving the capability of an integrated CA-Markov model to simulate spatio-temporal urban growth trends using an Analytical Hierarchy Process and Frequency Ratio,” *International Journal of Applied Earth Observation and Geoinformation*, vol. 59, pp. 65–78, Jul. 2017, doi: 10.1016/j.jag.2017.03.006.
[36] M. Jafari, H. Majedi, S. M. Monavari, A. A. Alesheikh, and M. K. Zarkesh, “Dynamic simulation of urban expansion through a CA-Markov model Case study: Hyrcanian region, Gilan, Iran,” *European Journal of Remote Sensing*, vol. 49, no. 1, pp. 513–529, Jan. 2016, doi: 10.5721/EuJRS20164927.